Available online at www.sciencedirect.com
ScienceDirect
Journal of Sound and Vibration 298 (2006) 1019–1033
JOURNAL OF SOUND AND VIBRATION
www.elsevier.com/locate/jsvi

A method for calculating the spectrum of Lyapunov exponents by local maps in non-smooth impact-vibrating systems

L. Jin[a], Q.-S. Lu[a], E.H. Twizell[b,*]

[a]*School of Science, Beijing University of Aeronautics and Astronautics, Beijing 100083, PR China*
[b]*Department of Mathematical Sciences, Brunel University, Uxbridge, Middlesex UB8 3PH, UK*

Received 2 March 2005; received in revised form 30 May 2006; accepted 1 June 2006
Available online 8 August 2006

Abstract

A general calculation method of calculating the spectrum of Lyapunov exponents is presented for n-dimensional nonlinear non-smooth systems by using the Poincaré map method. The Poincaré map is constructed by means of local maps to avoid calculating the Jacobian matrices at non-smooth points. The calculation of the spectrum of Lyapunov exponents for impact-vibrating systems with rigid constraints is given in detail. This method can be generally applied to systems with rigid or flexible (that is, perfectly elastic) constraints. In order to show the validity of this method, the spectrums of Lyapunov exponents are calculated in a large range of parameters for two given dynamical systems with rigid constraints and used to predict the dynamic behaviour.

1. Introduction

In the investigation of nonlinear non-smooth impact-vibrating systems, the spectrum of Lyapunov exponents is an important tool for determining the dynamic characteristics, which is an exponential measure of average divergence or convergence of nearby orbits in the phase space. Many researches focussed on the calculation methods of the spectrum of Lyapunov exponents [1–3].

There have been many results for calculating the spectrum of Lyapunov exponents of smooth dynamical systems described by differential equations and discrete mapping systems [1,2]. Wolf et al. [3] presented the first algorithms to estimate the non-negative Lyapunov exponents from an experimental time series. On the other hand, for non-smooth systems (with discontinuities or piecewise smoothness), the calculation methods of the spectrum of Lyapunov exponents has not been fully developed because the Jacobian matrices make no sense at non-smooth points. Hence, the classical methods, which are based on the Oseledec theorem for calculating Lyapunov exponents in smooth dynamical systems, cannot be applied to non-smooth systems directly. In recent years, several methods for calculating the spectrum of Lyapunov exponents of specific dynamical systems with discontinuities have been proposed. For example, Stefanski [4] and Stefanski and Kapitaniak [5] estimated the largest Lyapunov exponent for mechanical systems with impact by using the properties of synchronization phenomenon. Galvanetto [6] presented some numerical techniques to compute

*Corresponding author. Tel.: +44 1895 265603; fax: +44 1895 269732.
E-mail address: e.h.twizell@brunel.ac.uk (E.H. Twizell).

0022-460X/$ - see front matter
doi:10.1016/j.jsv.2006.06.035

the Lyapunov exponents of some low-dimensional discontinuous maps implicitly defined in mechanical stick–slip systems by means of the classical discrete map algorithm. Müller [7] supplemented certain transitional conditions to the linearized equations at the instants of impacts and applied the classical calculation methods of Lyapunov exponents to non-smooth systems. For an impact oscillator and an impact-pair system, de Souza and Caldas [8] introduced the transcendental maps to describe the solutions of integrable differential equations between impacts, supplemented by transitions at the instants of impact. At the same time, the Jacobian matrix of the nth iteration of the transcendental map was converted into an upper right triangular matrix to ensure the convergence and precision in the calculation process. Hence, the classical calculation methods for the spectrum of Lyapunov exponents of smooth dynamical systems could be applied to non-smooth systems in this case. All of the above methods for calculating the Lyapunov exponents can, however, be applied only to some specific non-smooth systems or those supplemented by some transitional conditions, so their usage is limited.

In this paper, a more general method for calculating the spectrum of Lyapunov exponents of n-dimensional non-smooth dynamical systems is presented. The method is essentially based on local maps, which were first proposed by Nordmark [9] to reveal singularities near the grazing orbits in an impact oscillator, and can be used to construct the Poincaré map for the whole impact process to avoid problems with defining the Jacobian matrices at non-smooth points. It should be mentioned that there were a few more works of such attempts in the application of the local maps, for example [10]. The detailed procedures to construct the local maps for general impact-vibrating systems with rigid or flexible (that is, perfectly elastic) constraints, as well as the calculation of the spectrum of Lyapunov exponents, are demonstrated in Sections 2 and 3. The cases of Filippov (namely, sliding) solutions [11] or chattering with infinitely many impacts in finite time [12,13] are not considered here, however, and should be studied further. In order to show the validity of this method, the numerical simulations of the spectrum of Lyapunov exponents in a large range of parameters are successfully carried out in Section 4 for two given nonlinear dynamical systems with rigid constraints to predict their dynamic behaviour.

2. Calculation of the spectrum of Lyapunov exponents in impact-vibrating systems with rigid constraints

Consider the n-dimensional non-autonomous system

$$\dot{\mathbf{x}} = \mathbf{f}(\mathbf{x}, t), \quad \mathbf{x} \in \mathbf{R}^n, \ \ t \in \mathbf{R}^+, \tag{1}$$

where $\mathbf{f}$ is a smooth vector field, which is periodic with respect to time t and nonlinear with respect to $\mathbf{x}$. So, system (1) can be written as a $(n+1)$-dimensional autonomous system as follows:

$$\begin{aligned} &\dot{\mathbf{x}} = \mathbf{f}(\mathbf{x}, \varphi), \quad (\mathbf{x}, \varphi) \in \mathbf{R}^n \times S^1, \\ &\dot{\varphi} = \omega, \end{aligned} \tag{2}$$

where φ is the phase angle and ω is the angular frequency. Assume that the system has a rigid constraint.

Due to the existence of a rigid constraint, trajectories in the phase space are discontinuous at the instants of impact. Therefore, the Jacobian matrices of the system do not exist at discontinuous points, and then the method for calculating the spectrum of Lyapunov exponents of smooth dynamical systems cannot be applied to non-smooth impact-vibrating systems directly. In this paper, local maps of non-smooth systems are introduced in order to construct the Poincaré map first of all, and then the non-smooth impact-vibrating systems (2) is transformed into a discrete dynamical system by the Poincaré map method. Hence, one can calculate the spectrum of Lyapunov exponents of system (2) by using that of the discrete dynamical system. In this general way, the direct calculation of the Jacobian matrices of system (2) at discontinuous points can be avoided.

2.1. Construction of the Poincaré map by local maps

For the non-smooth impact-vibrating system (2) caused by rigid constraints, a constant phase supersurface is taken as the Poincaré section defined by

$$\Pi^{\varphi_c} = \{(\mathbf{x}, \varphi) \in \mathbf{R}^n \times S^1 | \varphi = \varphi_c\} = \mathbf{R}^n \tag{3}$$

and the Poincaré map is

$$P : \Pi^{\varphi_c} \to \Pi^{\varphi_c}. \tag{4}$$

This map is composed of two sub-maps: one is the map of the impact process, and the other is the map of the non-impact process.

In the impact process, the rigid constraint surface (that is, the impact surface) Σ is defined by

$$\Sigma = \{(\mathbf{x}, \varphi) \in \mathbf{R}^n \times S^1 \,|\, h(\mathbf{x}, \varphi) = 0\} = \{(\mathbf{y}, \varphi) \in \mathbf{R}^{n-1} \times S^1\}, \tag{5}$$

where $\mathbf{y}$ represents the point on Σ.

According to the assumption of rigid impact, the relation for the states before impact and after impact of the system satisfies

$$\mathbf{y}_+ = -[\mathbf{r}]\mathbf{y}_-, \tag{6}$$

where the subscripts $-, +$ denote the values before and after impact, respectively, and $[\mathbf{r}]$ is the matrix of restitution, which can be used to describe the impact conditions.

In the non-impact process, the flow Φ_t is smooth. Due to the nonlinearity of the vector field with respect to the state variable $\mathbf{x}$, however, it is difficult to obtain the analytical solution of the flow Φ_t. One way is to resort to numerical methods (such as the Runge–Kutta method, etc.) to solve the following initial-value problem in the region without impact

$$\begin{aligned} &\dot{\mathbf{x}} = \mathbf{f}(\mathbf{x}, \varphi), \quad (\mathbf{x}, \varphi) \in \mathbf{R}^n \times S^1 \backslash \Sigma, \\ &\mathbf{x}(\varphi_0) = \mathbf{x}_0, \end{aligned} \tag{7}$$

where $\mathbf{x}_0$ is the initial condition.

In order to construct the Poincaré map P described by Eq. (4), suppose that a trajectory Γ of impact-vibrating system (2) contacts the rigid constraint surface Σ at the point O_c with the phase $\varphi = \varphi_c$, and leaves Σ at the point O'_c with the same phase $\varphi = \varphi_c$ since the impact is instantaneous from the rigid constraint assumption. Fig. 1 shows the situation of the trajectory Γ crossing the Poincaré section Π^{φ_c} in the state–space $\mathbf{R}^n \times S^1$.

Taking account of the fact that the impact process takes place on the constraint surface Σ with the singularities of the flow Φ_t, we consider the local maps defined by the flow near the constraint surface. The surface Σ is divided into two parts: the incidence part Σ^- with the normal velocity $v<0$ (that is, moving toward the surface) and the reflection part Σ^+ with the normal velocity $v>0$ (that is, rebounding from the surface).

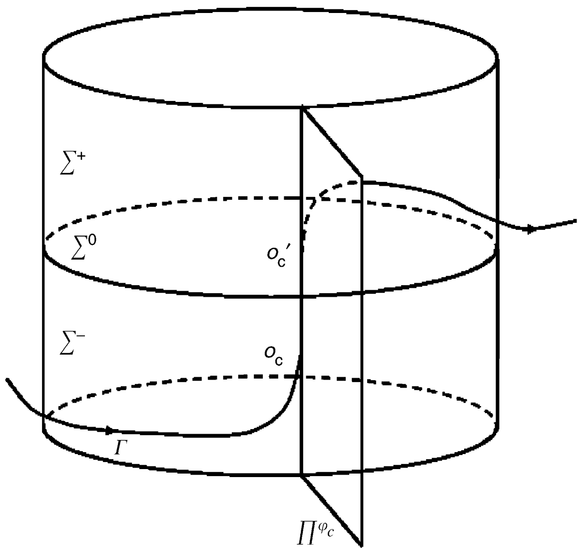

Fig. 1. A trajectory crosses the Poincaré section Π^{φ_c} and the rigid constraint surface Σ.

According to the situation of the trajectory Γ intersecting with the rigid constraint surface Σ, three kinds of local maps are defined: (I) a projection map P_I from the constant phase section Π^{φ_c} near the point O_c to the constraint section Σ^- ; (II) an impact map P_{II} from the constraint section Σ^- to the constraint section Σ^+; (III) a projection map P_{III} from the constraint section Σ^+ to the constant phase section Π^{φ_c} near the point O_c'.

In general, these local maps are related to switches between different states in the impact process, so they are the switch transforms of the state variables. Now consider the above three local maps with their Jacobian matrices in detail.

(I) *The map P_I and its Jacobian matrix*: Let $\mathbf{z} = (\mathbf{x}, \varphi)^{\mathrm{T}} \in \mathbf{R}^n \times S^1$, $\mathbf{F}(\mathbf{z}) = (\mathbf{f}(\mathbf{z}), \omega)^{\mathrm{T}}$ be the vector field in the state space $\mathbf{R}^n \times S^1$, and let $h(\mathbf{z}) = 0$ be the equation of the rigid constraint surface Σ (that is, the switch surface). Define an $(n+1)$-dimensional switch map $P_L : \Pi^{\varphi_c} \to \Sigma^-$, $\mathbf{z} \mapsto P_L(\mathbf{z})$ near the point O_c, given by the flow Φ_t of system (2). Using the geometrical relationship between the trajectory and the switch surface under the transversality condition, one can deduce a general formula for calculating the Jacobian matrix of P_L at the point O_c as follows [10]:

$$\mathrm{D}P_L(\mathbf{z}_c) = \mathbf{I} - \frac{\mathbf{F}(\mathbf{z}_c)\mathrm{D}h(\mathbf{z}_c)}{\mathrm{D}h(\mathbf{z}_c) \bullet \mathbf{F}(\mathbf{z}_c)}, \tag{8}$$

where the point O_c corresponds to $\mathbf{z}_c = (\mathbf{x}_{\varphi_c -}, \varphi_c)$, $\mathbf{I}$ is the $(n+1)$-dimensional identical matrix, $\mathbf{F}(\mathbf{z}_c)\mathrm{D}h(\mathbf{z}_c)$ is a second-order tensor, and $\mathrm{D}h(\mathbf{z}_c) \bullet \mathbf{F}(\mathbf{z}_c)$ is a scalar product of vectors.

The n-dimensional local map

$$P_I : \Pi^{\varphi_c} \to \Sigma^-, \quad \mathbf{x}_{\varphi_c -} \mapsto (\mathbf{y}_-, \varphi_c) \tag{9}$$

is just the restriction of the switch map P_L on the constraint section Σ^-. Therefore, by reserving the rows corresponding to the coordinates $(\mathbf{y}_-, \varphi_c)$ of the constraint section Σ^- and the columns corresponding to the coordinates $\mathbf{x}_{\varphi_c -}$ of the constant phase section Π^{φ_c} in the Jacobian matrix $\mathrm{D}P_L$ at the point $O_c(\mathbf{x}_{\varphi_c -}, \varphi_c)$ given by Eq. (8), the Jacobian matrix $\mathrm{D}P_I$ of the local map P_I can be expressed in an analytical way.

(II) *The map P_{II} and its Jacobian matrix*: The n-dimensional local map

$$P_{II} : \Sigma^- \to \Sigma^+, \quad (\mathbf{y}_-, \varphi_c) \mapsto (\mathbf{y}_+, \varphi_c) \tag{10}$$

can be given by the impact relation (6) and the instantaneous property, and its Jacobian matrix is

$$\mathrm{D}P_{II} = \begin{bmatrix} -\mathbf{r} & 0 \\ 0 & 1 \end{bmatrix} \tag{11}$$

(III) *The map P_{III} and its Jacobian matrix*: The n-dimensional local map

$$P_{III} : \Sigma^+ \to \Pi^{\varphi_c}, \quad (\mathbf{y}_+, \varphi_c) \mapsto \mathbf{x}_{\varphi_c +} \tag{12}$$

can be discussed as (I) by another similar switch map P_L'. The Jacobian matrix $\mathrm{D}P_{III}$ can be calculated by reserving the rows corresponding to the coordinates $\mathbf{x}_{\varphi_c +}$ of the constant phase section Π^{φ_c} and the columns corresponding to the coordinates $(\mathbf{y}_+, \varphi_c)$ of the constraint section Σ^+ in the Jacobian matrix $\mathrm{D}P_L'$ at the point $O_c'(\mathbf{x}_{\varphi_c +}, \varphi_c)$.

Now, one defines a compound map P_c to describe the impact process, constituted by the above three kinds of maps as

$$P_c = P_{III} \circ P_{II} \circ P_I \tag{13}$$

with the Jacobian matrix

$$\mathrm{D}P_c = \mathrm{D}P_{III} \circ \mathrm{D}P_{II} \circ \mathrm{D}P_I. \tag{14}$$

In the non-impact process, no trajectory goes through the constraint section Σ. In succession, one defines a n-dimensional map P_{IV} from the constant phase section Π^{φ_c} returning to Π^{φ_c} directly without impact, that is,

$$P_{IV} : \Pi^{\varphi_c} \to \Pi^{\varphi_c}, \quad \mathbf{x}_{\varphi_{c+}} \mapsto \mathbf{x}_{\varphi_{c-}}, \tag{15}$$

which is a smooth map (homeomorphism). Its Jacobian matrix $\mathrm{D}P_{IV}$ can be obtained by the differentiation rule of multivariate functions

$$\mathrm{D}P_{IV} = \left.\frac{\partial \mathbf{x}}{\partial \mathbf{x}_{\varphi_{c+}}}\right|_{\varphi=\varphi_{c-}}. \tag{16}$$

Because system (2) is nonlinear with respect to $\mathbf{x}$, it is difficult to obtain the analytical solution. The numerical solution of the Jacobian matrix $\mathrm{D}P_{IV}$ at $\varphi = \varphi_{c-}$ can, however, be obtained by solving the following initial-value problem

$$\begin{aligned} &\frac{\mathrm{d}}{\mathrm{d}t}\left[\frac{\partial \mathbf{x}}{\partial \mathbf{x}_{\varphi_{c+}}}\right] = \left.\frac{\partial \mathbf{f}}{\partial \mathbf{x}}\frac{\partial \mathbf{x}}{\partial \mathbf{x}_{\varphi_{c+}}}\frac{\partial \mathbf{x}}{\partial \mathbf{x}_{\varphi_{c+}}}\right|_{\varphi=\varphi_{c+}} = \mathbf{I}, \\ &\left.\frac{\partial \mathbf{x}}{\partial \mathbf{x}_{\varphi_{c+}}}\right|_{\varphi=\varphi_{c+}} = \mathbf{I} \end{aligned} \tag{17}$$

together with the initial-value problem (7) simultaneously.

The Poincaré map P defined by Eq. (4) can be expressed by a composition of the above maps

$$P = P_{IV} \circ P_{III} \circ P_{II} \circ P_I = P_{IV} \circ P_c \tag{18}$$

with the Jacobian matrix

$$\mathrm{D}P = \mathrm{D}P_{IV} \circ \mathrm{D}P_{III} \circ \mathrm{D}P_{II} \circ \mathrm{D}P_I = \mathrm{D}P_{IV} \circ \mathrm{D}P_c. \tag{19}$$

2.2. *Mathematical description of the spectrum of Lyapunov exponents of impact-vibrating systems with rigid constraints*

As shown before, the Poincaré map method is adopted by means of the Poincaré map P described in Eq. (4):

$$\mathbf{x}^{(k)} = P(\mathbf{x}^{(k-1)}), \quad \mathbf{x}^{(k-1)}, \mathbf{x}^{(k)} \in \Pi^{\varphi_c}, \ \ k \in \mathbf{Z}. \tag{20}$$

On the constant phase section Π^{φ_c}, one chooses two nearby points $\mathbf{x}^{(0)}$ and $\mathbf{x}^{(0)} + \delta\mathbf{x}^{(0)}$, from which originate the nearby orbits G_1 and G_2 of the discrete dynamical system (20). When $\delta\mathbf{x}^{(k-1)}$ is sufficiently small, the linearized equation of system (20) at the point $\mathbf{x}^{(0)}$ is given as follows:

$$\delta\mathbf{x}^{(k)} = \mathrm{D}P(\mathbf{x}^{(k-1)}) \cdot \delta\mathbf{x}^{(k-1)}, \tag{21}$$

where $\mathrm{D}P(\mathbf{x}^{(k-1)})$ is the Jacobian matrix of Eq. (20) at the point $\mathbf{x}^{(k-1)}$.

According to formulae (20) and (21), one obtains

$$\delta\mathbf{x}^{(k)} = \mathrm{D}P^k(\mathbf{x}^{(0)}) \cdot \delta\mathbf{x}^{(0)}, \tag{22}$$

where

$$\mathrm{D}P^k(\mathbf{x}^{(0)}) = \mathrm{D}P(\mathbf{x}^{(k-1)}) \cdot \mathrm{D}P(\mathbf{x}^{(k-2)}) \cdots \mathrm{D}P(\mathbf{x}^{(0)}) \tag{23}$$

then the spectrum of Lyapunov exponents of the discrete dynamical systems (20) is defined as [2]

$$\lambda_i = \lim_{k\to\infty} \frac{1}{k} \ln |m_i^{(k)}| \quad (i = 1, 2, \ldots, n), \tag{24}$$

where $m_i^{(k)}$ $(i = 1, 2, \ldots, n)$ are the ith eigenvalues of the Jacobian matrix $\mathrm{D}P^k(\mathbf{x}^{(0)})$ of the n-dimensional Poincaré map P at the point $\mathbf{x}^{(0)}$.

In calculating the spectrum of Lyapunov exponents directly according to (24), one needs firstly the Jacobian matrix $\mathrm{D}P^k(\mathbf{x}^{(0)})$ of the Poincaré map P. In the iterative process of calculating $\mathrm{D}P^k(\mathbf{x}^{(0)})$, however, morbid problems may be encountered in which some elements of $\mathrm{D}P^k(\mathbf{x}^{(0)})$ become either very large for chaotic attractors or null for periodic attractors. This makes the numerical computation results unreliable.

To prevent this computation problem, formula (24) cannot be used directly. In this paper, we compute the average exponent divergence rate between the basis orbit beginning at the point $\mathbf{x}^{(0)}$ and its nearby orbit along the direction of $\mathbf{u}^{(0)} = \delta\mathbf{x}^{(0)}/\|\delta\mathbf{x}^{(0)}\|$ by the following formula:

$$\lambda(\mathbf{x}^{(0)}, \mathbf{u}^{(0)}) = \lim_{k\to\infty} \frac{1}{k} \ln \frac{\|\delta\mathbf{x}^{(k)}\|}{\|\delta\mathbf{x}^{(0)}\|}, \tag{25}$$

where $\|\delta\mathbf{x}^{(k)}\|$ is the norm of $\delta\mathbf{x}^{(k)}$ $(k = 0, 1, \ldots)$. If choosing n linearly independent vectors $\mathbf{e}_i : (i = 1, 2, \ldots, n)$, for example, the eigenvectors of the matrix $\mathrm{D}P(\mathbf{x}^{(0)})$ as the iterative initial values $\mathbf{u}^{(0)}$, one can obtain n values of $\lambda_i(\mathbf{x}^{(0)}, \mathbf{e}_i)$ $(i = 1, 2, \ldots, n)$ by Eq. (25) ranked from small to large as

$$\lambda_1 \geqslant \lambda_2 \geqslant \cdots \geqslant \lambda_n \tag{26}$$

which are named the spectrum of Lyapunov exponents of the discrete dynamical system (20) and the non-smooth impact-vibrating system (1) with rigid constraint as well.

2.3. Calculation of the spectrum of Lyapunov exponents of impact-vibrating systems with rigid constraints

Choose $\mathbf{x}^{(0)} \in \Pi^{\varphi_c}$ and n linearly independent initial perturbations $(\delta\mathbf{x}_1^{(0)}, \delta\mathbf{x}_2^{(0)}, \ldots, \delta\mathbf{x}_n^{(0)})$, such as the eigenvectors of $\mathrm{D}P(\mathbf{x}^{(0)})$. According to the non-smooth characteristics of the nonlinear dynamical system with rigid constraint and introducing the local maps, one can obtain the Jacobian matrix $\mathrm{D}P$ of the Poincaré map P by Eq. (19). Then, one iterates the linearization equation (21). For the kth iteration, the difference between two nearby orbits is $(\delta\mathbf{x}_1^{(k)}, \delta\mathbf{x}_2^{(k)}, \ldots, \delta\mathbf{x}_n^{(k)})$. This iteration process is given as follows. Considering the existence of rigid constraint in this system, the iterations are made from a constant phase section Π^{φ_c} just before the impact, and $(\mathbf{u}_1^{(0)}, \mathbf{u}_2^{(0)}, \ldots, \mathbf{u}_n^{(0)}) = (\delta\mathbf{x}_1^{(0)}/\|\delta\mathbf{x}_1^{(0)}\|, \delta\mathbf{x}_2^{(0)}/\|\delta\mathbf{x}_2^{(0)}\|, \ldots, \delta\mathbf{x}_n^{(0)}/\|\delta\mathbf{x}_n^{(0)}\|)$ is defined. Then, taking $(\mathbf{u}_1^{(0)}, \mathbf{u}_2^{(0)}, \ldots, \mathbf{u}_n^{(0)})$ as the initial vector and introducing the local maps, $(\mathbf{u}_1^{(0)}, \mathbf{u}_2^{(0)}, \ldots, \mathbf{u}_n^{(0)})$ is mapped onto the same constant phase section Π^{φ_c} by the Jacobian matrices $\mathrm{D}P_c$ given by Eq. (14) just after the impact. Then, this point is mapped onto the constant phase section Π^{φ_c} again by the Jacobian matrix $\mathrm{D}P_{IV}$ given by Eq. (16) to obtain the n-dimensional vectors $(\delta\mathbf{x}_1^{(1)}, \delta\mathbf{x}_2^{(1)}, \ldots, \delta\mathbf{x}_n^{(1)})$, where $\delta\mathbf{x}_i^{(1)} = \delta\mathbf{x}(1; \mathbf{u}_i^{(0)}, \mathbf{x}^{(0)}) = \mathrm{D}P(\mathbf{x}^{(0)})\mathbf{u}_i^{(0)}$, $(i = 1, 2, \ldots, n)$. Using the Gram–Schmidt ortho-normalization for the vectors $(\delta\mathbf{x}_1^{(1)}, \delta\mathbf{x}_2^{(1)}, \ldots, \delta\mathbf{x}_n^{(1)})$, gives the vectors $(\mathbf{u}_1^{(1)}, \mathbf{u}_2^{(1)}, \ldots, \mathbf{u}_n^{(1)})$ used as the initial value of the next iteration. The next iteration proceeds in the same way. In general, the n-dimensional vectors $(\delta\mathbf{x}_1^{(k)}, \delta\mathbf{x}_2^{(k)}, \ldots, \delta\mathbf{x}_n^{(k)})$ are obtained after the kth iteration. The result of Gram–Schmidt ortho-normalization can be described as follows:

$$\begin{aligned}
\mathbf{v}_1^{(k)} &= \delta\mathbf{x}_1^{(k)} \\
\mathbf{u}_1^{(k)} &= \mathbf{v}_1^{(k)}/\|\mathbf{v}_1^{(k)}\| \\
\mathbf{v}_2^{(k)} &= \delta\mathbf{x}_2^{(k)} - \langle\delta\mathbf{x}_2^{(k)}, \mathbf{u}_1^{(k)}\rangle\mathbf{u}_1^{(k)} \\
\mathbf{u}_2^{(k)} &= \mathbf{v}_2^{(k)}/\|\mathbf{v}_2^{(k)}\| \\
&\vdots \\
\mathbf{v}_n^{(k)} &= \delta\mathbf{x}_n^{(k)} - \langle\delta\mathbf{x}_n^{(k)}, \mathbf{u}_1^{(k)}\rangle\mathbf{u}_1^{(k)} - \cdots - \langle\delta\mathbf{x}_n^{(k)}, \mathbf{u}_{n-1}^{(k)}\rangle\mathbf{u}_{n-1}^{(k)} \\
\mathbf{u}_n^{(k)} &= \mathbf{v}_n^{(k)}/\|\mathbf{v}_n^{(k)}\|,
\end{aligned} \tag{27}$$

where $\|\mathbf{v}_i^{(k)}\|$ $(i = 1, 2, \ldots, n)$ is the norm of $\mathbf{v}_i^{(k)}$, $\langle\delta\mathbf{x}_j^{(k)}, \mathbf{u}_j^{(k)}\rangle$ $(i,j = 1, 2, \ldots, n)$ is the standard scalar product.

The vectors $(\mathbf{u}_1^{(k)}, \mathbf{u}_2^{(k)}, \ldots, \mathbf{u}_n^{(k)})$ are normalized and orthogonal to each other, and the subspace spanned by $(\mathbf{u}_1^{(k)}, \mathbf{u}_2^{(k)}, \ldots, \mathbf{u}_n^{(k)})$ is the same as that spanned by $(\delta\mathbf{x}_1^{(0)}, \delta\mathbf{x}_2^{(0)}, \ldots, \delta\mathbf{x}_n^{(0)})$; $(\mathbf{u}_1^{(k)}, \mathbf{u}_2^{(k)}, \ldots, \mathbf{u}_n^{(k)})$ can be chosen as the initial value of the $(k+1)$th iteration. A general relation can be deduced as follows:

$$\delta\mathbf{x}_i^{(k)} = \delta\mathbf{x}(k; \delta\mathbf{x}_i^{(0)}, \mathbf{x}^{(0)}) = \|\mathbf{v}_i^{(k)}\|\|\mathbf{v}_i^{(k-1)}\| \cdots \|\mathbf{v}_i^{(1)}\|\mathbf{u}_i^{(k)} \quad (i = 1, 2, \ldots, n). \tag{28}$$

Applying formula (25), one can approximately obtain the spectrum of Lyapunov exponents of nonlinear dynamical systems with rigid constraint for K sufficiently large as

$$\begin{aligned}\lambda_i &\approx \frac{1}{K}\ln\|\delta\mathbf{x}(K;\delta\mathbf{x}^{(0)},\, \mathbf{x}^{(0)})\| \\ &= \frac{1}{K}\ln\prod_{k=1}^{K}\|\mathbf{v}_i^{(k)}\| \\ &= \frac{1}{K}\sum_{k=1}^{K}\ln\|\mathbf{v}_i^{(k)}\| \quad (i=1,2,\ldots,n). \end{aligned} \tag{29}$$

3. Calculation of the spectrum of Lyapunov exponents in impact-vibrating systems with flexible constraints

If the vector field of system (2) has a flexible (that is, perfectly elastic) constraint, which is nonlinear with respect to $\mathbf{x}$, and assuming that there is no damping, sliding or Filippov solution [11] taking place, then the flow is continuous but piecewise smooth between the impact and non-impact processes. Therefore, the Jacobian matrices do not exist at the impact points in this case, and the method for calculating the spectrum of Lyapunov exponents of smooth dynamical systems cannot be applied directly.

To avoid calculating the Jacobian matrices of vector fields at the impact points, the Poincaré map method is still used to transform the piecewise smooth dynamical system (2) into a discrete dynamical system. At the same time, one considers that the coordinates of the constant phase section Π^{φ_c} can be used as the state variables both in the impact and the non-impact processes. Hence, one can take the constant phase section Π^{φ_c} before impact as the Poincaré section, and define the Poincaré map P by Eq. (4). It is obvious that the local map P_c is just the identity map I in this case. The flow of system (2) is continuous now, and its Poincaré map P can be decomposed of two continuous flow maps in the impact and non-impact processes, respectively, as follows:

$$P = P_{\mathrm{non}} \circ P_{\mathrm{flex}}, \tag{30}$$

where P_{non} is defined as the continuous flow map in the non-impact process, and P_{flex} is defined as another continuous flow map in the process of contacting flexible constraints. The Jacobian matrix $\mathrm{D}P$ can be expressed as

$$\mathrm{D}P = \mathrm{D}P_{\mathrm{non}} \circ \mathrm{D}P_{\mathrm{flex}}, \tag{31}$$

where the Jacobian matrices $\mathrm{D}P_{\mathrm{non}}$ and $\mathrm{D}P_{\mathrm{flex}}$ can be calculated similarly by Eq. (16). Then the spectrum of Lyapunov exponents of nonlinear dynamical systems with flexible (perfectly elastic) constraints can be obtained by Eq. (29).

It should be noted that if system (2) has damping, sliding or Filippov solution, the method for calculating the spectrum of Lyapunov exponents of system (2) is much more complex and will be the subject of future work.

4. Examples

4.1. Impact oscillator

An impact-vibrating system, as shown in Fig. 2, is composed of an oscillator attached to a linear spring and a rigid constraint. When the displacement x reaches a fixed value x_c, an impact will occur between the oscillator and the rigid constraint. The system is excited by an external periodic force, and the dimensionless equation of motion is

$$\ddot{x} + x = \beta\cos\omega t \quad (x<x_c), \tag{32}$$

which can be written as the following dynamical system:

$$\begin{bmatrix}\dot{x}\\ \dot{v}\\ \dot{\varphi}\end{bmatrix} = \begin{bmatrix} v\\ -x+\beta\cos\varphi \\ \omega\end{bmatrix} \quad (x<x_c), \tag{33}$$

where β, ω are the amplitude and the frequency of the external force, respectively.

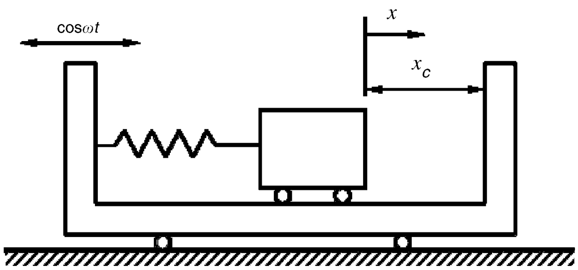

Fig. 2. An impact-vibrating system with an oscillator and a rigid constraint.

According to the rigid impact assumption, the relation between the states before and after impact at $x = x_c$ is

$$\begin{bmatrix} v \\ \varphi \end{bmatrix}_+ = \begin{bmatrix} -r & 0 \\ 0 & 1 \end{bmatrix} \begin{bmatrix} v \\ \varphi \end{bmatrix}_-, \tag{34}$$

where the subscripts $-, +$ denote the states before and after impact, respectively; r is the restitution coefficient.

Applying the Poincaré map method, one takes the constant phase section Π^{φ_c} before impact as the Poincaré section. The Jacobian matrix $\mathrm{D}P$ of the Poincaré map P of this impact vibration system can be given by Eq. (19), that is,

$$\mathrm{D}P = \mathrm{D}P_{IV} \circ \mathrm{D}P_c, \tag{35}$$

where the analytical expression of the Jacobian matrix $\mathrm{D}P_c$ of the compound map P_c is

$$\begin{aligned} \mathrm{D}P_c &= \mathrm{D}P_{III} \circ \mathrm{D}P_{II} \circ \mathrm{D}P_I \\ &= \begin{bmatrix} 0 & -\dfrac{v_+}{\omega} \\ 1 & \dfrac{x_+ - \beta\cos\varphi_+}{\omega} \end{bmatrix} \cdot \begin{bmatrix} -r & 0 \\ 0 & 1 \end{bmatrix} \cdot \begin{bmatrix} \dfrac{x_- - \beta\cos\varphi_-}{v_-} & 1 \\ -\dfrac{\omega}{v_-} & 0 \end{bmatrix} \\ &= \begin{bmatrix} -r & 0 \\ \dfrac{(1+r)(-x_- + \beta\cos\varphi_-)}{v_-} & -r \end{bmatrix}. \end{aligned} \tag{36}$$

The numerical solution of the Jacobian matrix $\mathrm{D}P_{IV}$ of the map P_{IV} follows by integrating Eqs. (17) and (33) numerically. Then the semi-analytical solution of the Jacobian matrix $\mathrm{D}P$ is obtained by Eq. (35). By means of the Jacobian matrix $\mathrm{D}P$, one iterates the linearized equation given by Eq. (21). When the iteration time is sufficiently large, the spectrum of Lyapunov exponents of Eq. (33) is obtained by Eq. (29).

When the parameters have the values $x_c = 0$, $\beta = 1.0$, $r = 0.8$, $\omega = 3.52$, the phase portrait of a single-impact period-1 attractor is shown in Fig. 3(a), and the test of the convergence of the iteration sequences of the spectrum of Lyapunov exponents is shown in Fig. 3(b). It is seen from Fig. 3(b) that there are two negative Lyapunov exponents. Their values are so close, however, that they cannot be distinguished clearly in this figure. This attractor is a periodic attractor. For this iteration sequences, 25,000 iterations were taken of which the first 2000 iterations are omitted as the transient process. The convergence of this iteration process with good precision is shown in Fig. 3(b).

When the parameters have the values $x_c = 0$, $\beta = 1.0$, $r = 0.8$, $\omega = 4.85$, the phase portrait of a chaotic attractor is shown in Fig. 4(a), and the test of the convergence of the iteration sequences of the spectrum of Lyapunov exponents is shown in Fig. 4(b). From Fig. 4(b), it can be seen that there exists a positive Lyapunov exponent, so this attractor is a chaotic attractor.

For further validating the correctness in the iteration process of the general method for calculating the spectrum of Lyapunov exponents in this paper, the bifurcation diagram of system (33) for the bifurcation parameter ω changing from 2.5 to 5.5 and the corresponding Lyapunov exponents diagram

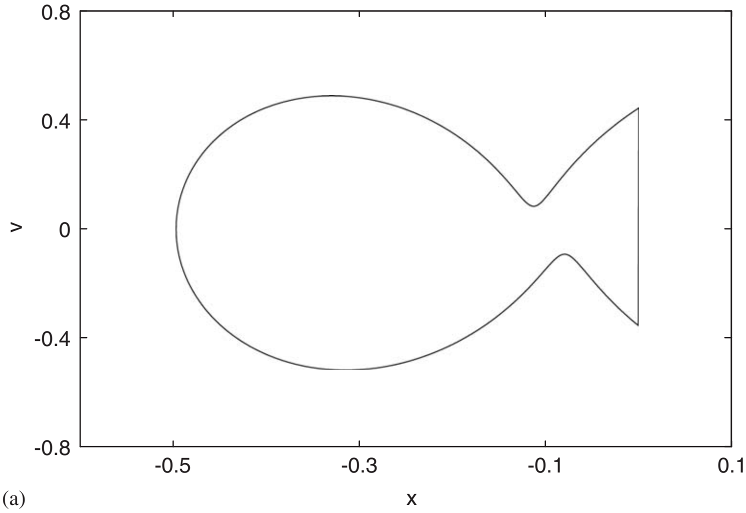

(a)

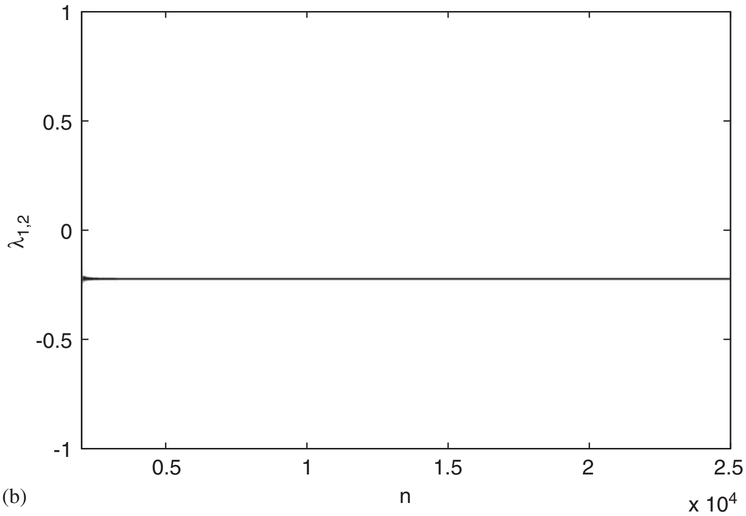

(b)

Fig. 3. (a) The phase portrait of a single-impact period-1 attractor and (b) convergent sequences in the iteration process of the spectrum of Lyapunov exponents of the periodic attractor.

are given in Figs. 5(a) and (b), respectively. In these figures, the increment of parameter ω is taken as 0.002 generally; it is reduced to about 0.0001, however, near the bifurcation point for higher accuracy. Comparing with Figs. 5(a) and (b), one can see that the regions where all Lyapunov exponents are negative correspond to periodic attractors, and that with at least one positive Lyapunov exponent correspond to chaotic attractors. And the same time, when the periodic solutions encounter bifurcations, the largest Lyapunov exponent is equal to zero from Fig. 5(b), for example, $\omega = 2.6534$, 2.968, 3.140, 3.338, 3.474, 4.642, 5.344, 5.480, etc.

Ref. [8] presented the bifurcation diagram of system (33) with the bifurcation parameter ω varying in a wide range from 2.0 to 5.0 and the corresponding Lyapunov exponents diagram by introducing a transcendental map. The method in Ref. [8] has its own limitation and then can only be applied to some special non-smooth systems. Moreover, the chaotic attractors appearing in the region of $\omega = 3.46$–3.464 were not reflected in its bifurcation diagram in Ref. [8], and the corresponding largest Lyapunov exponent in Ref. [8] was less than zero in its Lyapunov exponents diagram, which may be a result of the increment in the bifurcation parameter ω being too large. Therefore, when comparing with the method in Ref. [8], the method for calculating the

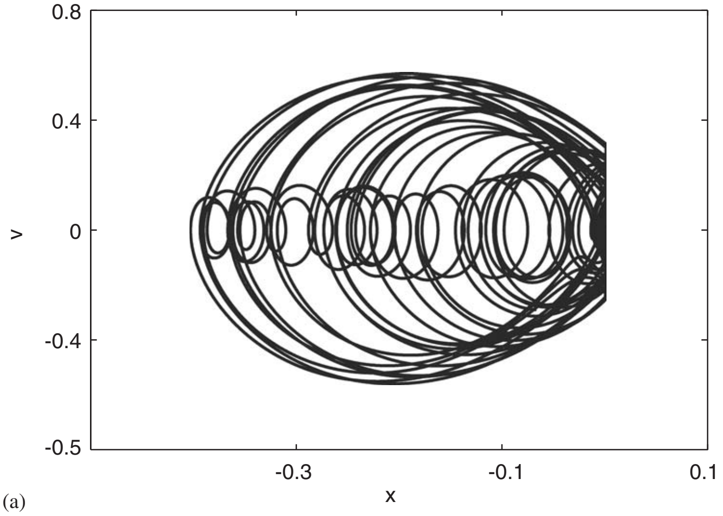

(a)

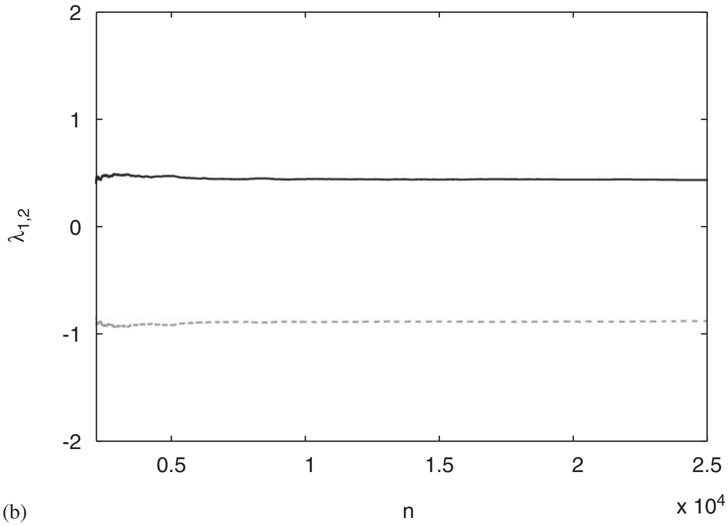

(b)

Fig. 4. (a) The phase portrait of a chaotic attractor and (b) convergent sequences in the iteration process of the spectrum of Lyapunov exponents of the chaotic attractor.

spectrum of Lyapunov exponents of non-smooth nonlinear dynamical systems given in this paper, not only can be used in a general extent of non-smooth dynamical systems, but also keeps high precision and convenience in computation.

4.2. An impact single pendulum

An impact-vibrating system, as shown in Fig. 6, is composed of a single pendulum OA in the perpendicular plane, with a mass m at the tip A, and a rigid constraint surface. A revolving flexible spring and a linear damper are set at the point O, and the pendulum is forced by a periodic external moment. Let the dimensionless angle between the pendulum and plumb line be x. Impacts occur between the pendulum and the rigid constraint when the dimensionless horizontal displacement between the pendulum tip A and the hanging point O reaches Δ. The dimensionless motion equation is

$$\ddot{x} + 2\delta\dot{x} - x + x^3 + g_1 \sin x = \beta \cos \omega t, \quad (\sin x < \Delta) \tag{37}$$

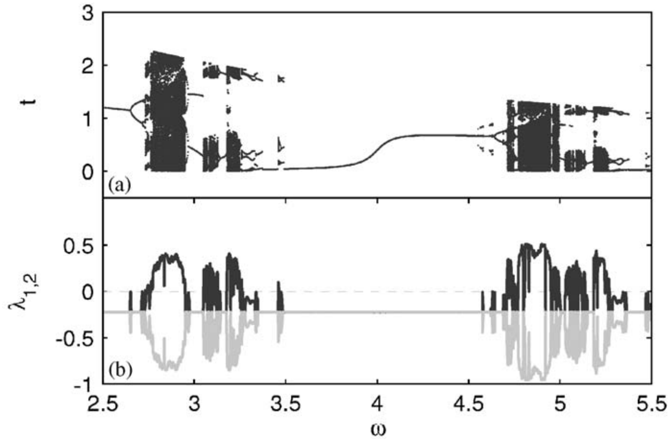

Fig. 5. (a) The bifurcation diagram of system (32) with respect to the parameter ω and (b) variation of the Lyapunov exponents with respect to the parameter ω.

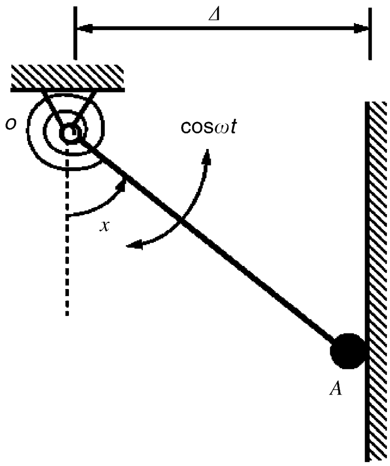

Fig. 6. An impact-vibrating system with a pendulum and a rigid constraint.

which can be written as

$$\begin{bmatrix} \dot{x} \\ \dot{v} \\ \dot{\varphi} \end{bmatrix} = \begin{bmatrix} v \\ -2\delta v + (x - x^3) - g_1 \sin x + \beta \cos \varphi \\ \omega \end{bmatrix}, \quad (\sin x < \Delta), \tag{38}$$

where β is the forcing amplitude, ω is the forcing frequency, δ is the linear damping coefficient, and g_1 is the dimensionless gravitation acceleration.

An impact occurs when $\sin x = \Delta$ under the relation

$$\begin{bmatrix} v \\ \varphi \end{bmatrix}_+ = \begin{bmatrix} -r & 0 \\ 0 & 1 \end{bmatrix} \begin{bmatrix} v \\ \varphi \end{bmatrix}_- . \tag{39}$$

Applying the Poincaré map method, the Jacobian matrix $\mathrm{D}P$ of the Poincaré map P of the impact-vibrating system is given by Eq. (19) as

$$\mathrm{D}P = \mathrm{D}P_{IV} \circ \mathrm{D}P_c, \tag{40}$$

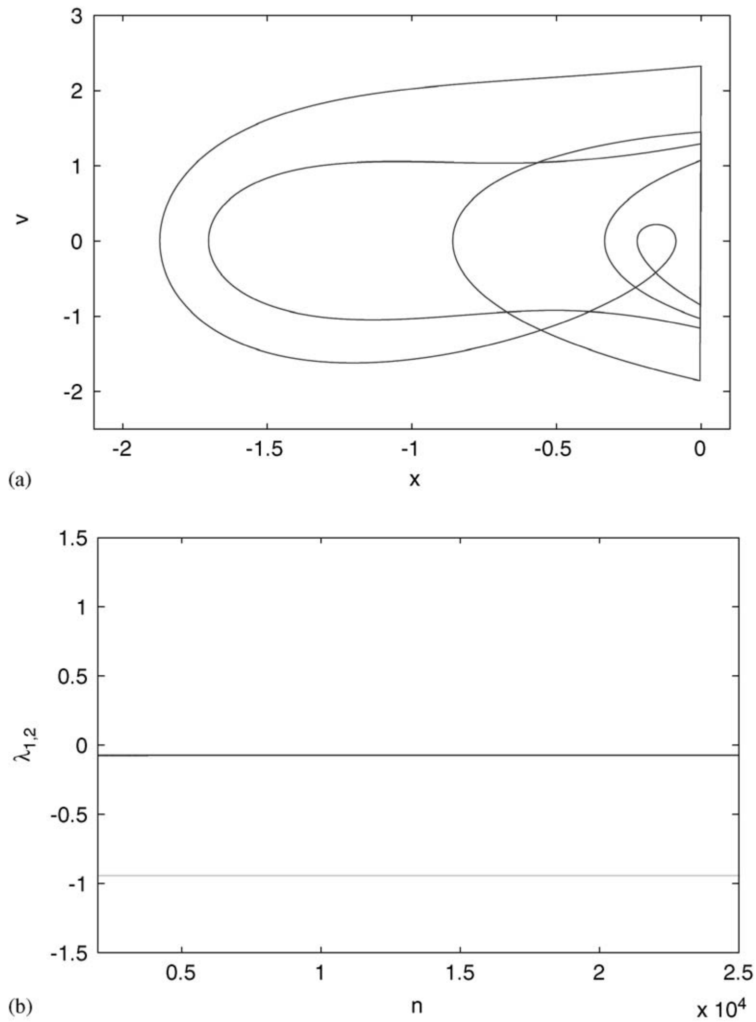

Fig. 7. (a) The phase portrait of a four-impact period-4 attractor and (b) convergent sequence in the iteration process of the spectrum of Lyapunov exponents of the periodic attractor.

where

$$
\begin{aligned}
\mathrm{D}P_c &= \mathrm{D}P_{III} \circ \mathrm{D}P_{II} \circ \mathrm{D}P_I, \\
&= \begin{bmatrix} 0 & -\dfrac{v_+}{\omega} \\ 1 & \dfrac{2\delta v_+ - (x_+ - x_+^3) + g_1 \sin x_+ - \beta \cos \varphi_+}{\omega} \end{bmatrix} \cdot \begin{bmatrix} -r & 0 \\ 0 & 1 \end{bmatrix} \\
&\quad \times \begin{bmatrix} \dfrac{2\delta v_+ - (x_+ - x_+^3) + g_1 \sin x_+ - \beta \cos \varphi_+}{\omega} & 1 \\ -\dfrac{\omega}{v_-} & 0 \end{bmatrix}, \\
&= \begin{bmatrix} -r & 0 \\ a_{21} & -r \end{bmatrix}
\end{aligned}
\tag{41}
$$

and $a_{21} = (1 + r)(x_- - x_-^3 - g_1 \sin x_- + \beta \cos \varphi_-)/v_-$

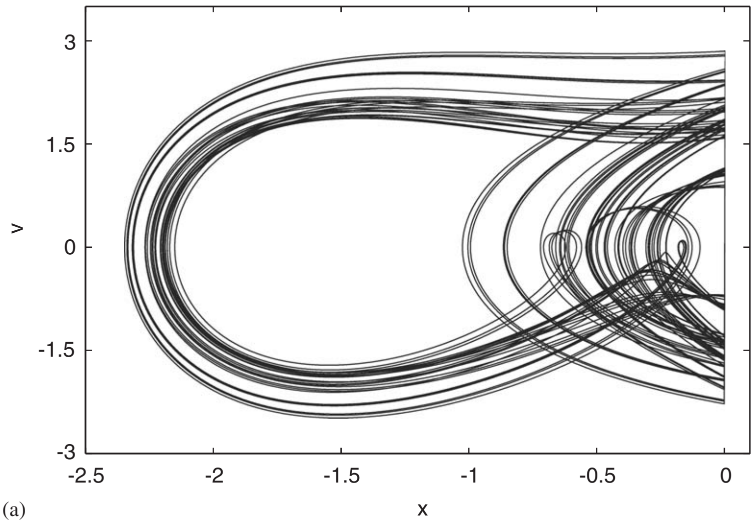

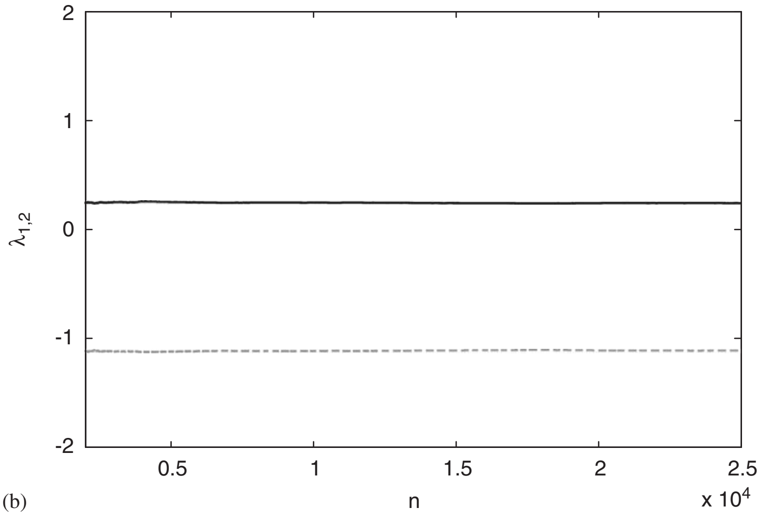

Fig. 8. (a) The phase portrait of a chaotic attractor and (b) convergent sequence in the iteration process of the spectrum of Lyapunov exponents of the chaotic attractor.

Integrating Eqs. (17) and (38) yields the Jacobian matrix $\mathrm{D}P_{IV}$ numerically. Then the semi-analytical solution of the Jacobian matrix $\mathrm{D}P$ of map P can be obtained by Eq. (40), and the spectrum of Lyapunov exponents of system (38) by formula (29).

With the parameters values $\varDelta = 0$, $\delta = 1.0$, $g_1 = 1.0$, $\omega = 1.1$, $r = 0.8$, $\beta = 1.91$, the phase portrait of a four-impact period-4 attractor is shown in Fig. 7(a). There are two negative Lyapunov exponents in Fig. 7(b), so that this attractor is a periodic attractor. The convergence of iteration with good precision is shown in Fig. 7(b).

When the parameters $\varDelta = 0$, $\delta = 1.0$, $g_1 = 1.0$, $\omega = 1.1$, $r = 0.8$, $\beta = 3.5$, the phase portrait of a chaotic attractor is shown in Fig. 8(a). There is one positive Lyapunov exponent in Fig. 8(b), so this attractor is a chaotic attractor.

The bifurcation diagram of system (38) for the bifurcation parameter β from 1.0 to 4.0 is given in Fig. 9(a), and the corresponding Lyapunov exponents diagram is given in Fig. 9(b). It is seen that all Lyapunov exponents are negative for periodic attractors and there is one positive Lyapunov exponents for chaotic attractors.

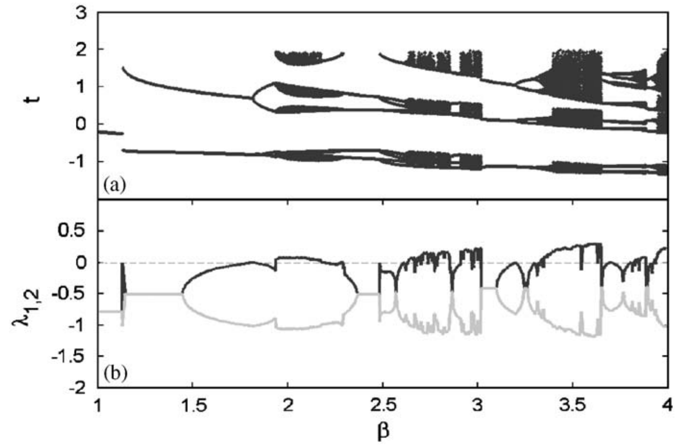

Fig. 9. (a) The bifurcation diagram of system (38) with respect to the parameter β and (b) variation of the Lyapunov exponents with respect to the parameter β.

At the same time, when the bifurcations of periodic solutions occur, their largest Lyapunov exponents are equal to zero in Fig. 9(b), that is, at $\beta = 1.13061$, 1.818, 2.182, 2.48447, 2.612, 3.198, 3.302, 3.700, 3.804, 3.912, etc.

5. Conclusion

Through analysing nonlinear, non-smooth, impact-vibrating systems, a general calculation method of the spectrum of Lyapunov exponents has been presented in this paper by using the Poincaré map method. The local maps in the impact process were introduced in order to avoid the difficulties in the calculation of the Jacobian matrix of the Poincaré map which does not exist at the non-smooth points. This method can be applied generally to n-dimensional non-smooth impact-vibrating systems with rigid constraints or flexible (that is, perfectly elastic) constraints. As examples, the corresponding spectrum of Lyapunov exponents are given for two given nonlinear, impact-vibrating systems with rigid constraints. In order to show the validity of the above universal method, the spectra of Lyapunov exponents in a large range of parameters were calculated for these systems, and the results compared with the bifurcation diagrams obtained by the Poincaré map method in the corresponding parameter range.

Acknowledgments

The work was supported by the National Natural Science Foundation of China (no. 10572011, no. 10432010 and no. 10272008) and The Royal Society of London.

References

[1] V.I. Oseledec, A multiplicative ergodic theorem: Lyapunov characteristic numbers for dynamical systems, *Transactions of the Moscow Mathematical Society* 19 (1968) 197–231.
[2] T.S. Parker, *Practical Numerical Algorithms for Chaotic Systems*, Springer, New York, 1989.
[3] A. Wolf, J.B. Swift, H.L. Swinney, J.A. Vastano, Determining Lyapunov exponents from a time series, *Physica D* 16 (1985) 285–317.
[4] A. Stefanski, Estimation of the largest Lyapunov exponent in systems with impacts, *Chaos, Solitons & Fractals* 11 (2000) 2443–2451.
[5] A. Stefanski, T. Kapitaniak, Estimation of the dominant Lyapunov exponent of non-smooth systems on the basis of maps synchronization, *Chaos, Solitons & Fractals* 15 (2003) 233–244.
[6] U. Galvanetto, Numerical computation of Lyapunov exponents in discontinuous maps implicitly defined, *Computer Physics Communications* 131 (2000) 1–9.
[7] P. Müller, Calculation of Lyapunov exponents for dynamics systems with discontinuities, *Chaos, Solitons & Fractals* 5 (9) (1995) 1671–1681.

[8] S.L.T. de Souza, I.L. Caldas, Calculation of Lyapunov exponents in systems with impacts, *Chaos, Solitons & Fractals* 19 (2004) 569–579.
[9] A.B. Nordmark, Non-periodic motion caused by grazing incidence in an impact oscillator, *Journal of Sound and Vibration* 145 (2) (1991) 279–297.
[10] M. Oestreich, N. Hinrichs, K. Popp, Bifurcation and stability analysis for a non-smooth friction oscillator, *Archives of Applied Mechanics* 66 (1996) 301–314.
[11] A. Filippov, *Differential Equations with Discontinuous Righthand Side*, Kluwer Academic Publishers, Dordrecht, 1988.
[12] C. Budd, F. Dux, Chattering and related behavior in impact oscillators, *Philosophical Transactions of the Royal Society of London A* 347 (1999) 365–389.
[13] D.J. Wagg, S.R. Bishop, Chatter, sticking and chaotic impacting motion in a two-degree of freedom impact oscillator, *International Journal Bifurcation Chaos* 11 (2001) 57–71.